

## BRIEF COMMUNICATION

---

### COMPUTER SIMULATION OF THE EFFECT OF THE NODAL GAP RESISTANCE ON IONIC CURRENT MEASUREMENTS IN THE RANVIER NODE MEMBRANE

CORNELIA ZACIU, MIOARA TRIPȘA, AND V. VASILESCU, *Department of Biophysics,  
Faculty of Medicine, Bucharest, 76241 Romania*

**ABSTRACT** Results are presented of a computer simulation of the effect of the irreducible resistance introduced by the nodal gap, in series with the impedance of the axon membrane. A clamp potential is applied to a structure modeled as an electric circuit composed of a resistance in series with the membrane impedance, and modified nerve equations describing membrane currents are solved to predict the effect of nodal series resistance on these currents. These studies reveal changes in the absolute values and kinetics of the ionic currents (errors > 10–20%) for selected values of series resistance.

#### INTRODUCTION

Although voltage-clamp measurements have been performed for over 30 years on the giant axon (Marmont, 1949) and for over 20 years on the Ranvier node (Dodge and Frankenhaeuser, 1958), the effect of uncompensated series resistance has led to numerous errors in the measurements of the activation kinetics of ionic channels (Binstock et al., 1975) and gating currents (Moore, 1978). Though efforts were made to reduce this series resistance in the giant axon by a suitable placement of recording and stimulation electrodes, the effect could be totally compensated only by using an electronic circuit. But this electronic compensation too was found to be liable to errors as it depended on the rising time of the pulse applied for adjusting compensation (Binstock et al., 1975; Cole and Lecar, 1975).

Briefly, uncompensated series resistance or incorrect compensation of this resistance has the following effects: (a) changes in the absolute values of membrane currents; (b) changes in the kinetics of these currents; (c) changes in gating currents.

One of the major research goals today is to elucidate the molecular mechanisms of operation of the ionic channels in excitable membranes (Hille, 1978). For the above reason it has not been possible to learn whether or not, the same type of axons of various species, e.g., squid, *Loligo*, *Myxicola*, have the same activation kinetics of ionic channels (Binstock et al., 1975).

In the giant axon the problem of compensating the series resistance has been solved in

several practical ways by means of estimate and compensation (Binstock et al., 1975; Cole and Lecar, 1975). Although as far back as 1974 this problem was reported to be important for the study of the Ranvier node (Drouin and Neumcke, 1974) a possible compensation of the series resistance has neither theoretically nor practically been studied. This paper presents the results of a computer simulation of the effect of this resistance on voltage clamp measurements in the Ranvier node membrane.

# SOURCES OF THE SERIES RESISTANCE IN VOLTAGE CLAMP MEASUREMENTS ON THE RANVIER NODE MEMBRANE

Fig. 1 illustrates the difficulty of properly voltage clamping the nodal membrane when an external resistance is in series with the membrane impedance. This figure is a diagram of the equivalent circuit involved in voltage-clamp measurements on the myelinated fiber (Nonner, 1969), in which the series resistance due to the nodal gap is included.

The sources of this series resistance are the resistance of the nodal gap ( $R_s$ )—which may be considered as a microelectrode—and the resistance of the electrolyte solution between the fiber and the electrode  $A$  ( $R_A$ ) (Fig. 2). Of the total series resistance the nodal gap resistance is the largest fraction (Drouin and Neumcke, 1974).

Even though this resistance ( $R_s$ ) cannot be measured directly, a rough estimate can be

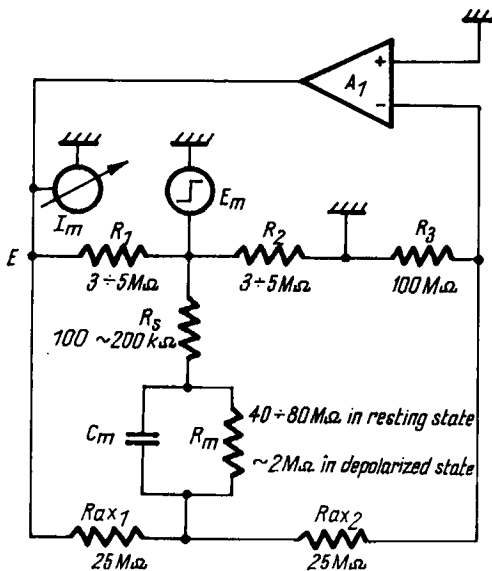


FIGURE 1

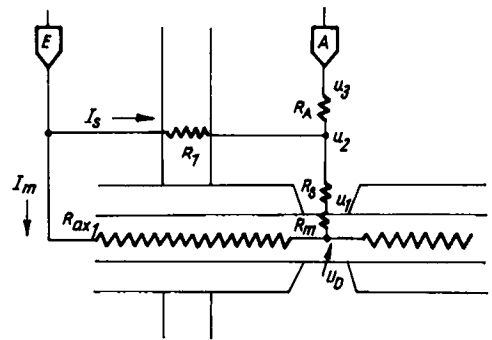


FIGURE 2

FIGURE 1 Equivalent diagram of voltage-clamp measurements on the myelinated fiber (according to Nonner's method, 1969); the series resistance due to the nodal gap is also included;  $R_1$ ,  $R_2$ , and  $R_3$  are the isolation resistances created by vaseline seals ( $R_1$  and  $R_2$ ) or by the air gap ( $R_3$ );  $R_{ax1}$  and  $R_{ax2}$  are the axoplasm resistances on adjacent internodes;  $C_m$  and  $R_m$  are the capacity and resistance of membrane.

FIGURE 2 Schematic diagram showing the connection of the nodal region in voltage-clamp measurements.  $R_s$  and  $R_A$  are irreducible series resistances (after Drouin and Neumcke, 1974).

obtained by considering the nodal gap as a cylinder between the isolating myelin sheaths (Drouin and Neumcke, 1974). Consequently,

$$R_s = \frac{1}{2\pi d\sigma} \ln \frac{r_1}{r_2} \tag{1}$$

where  $r_1$  and  $r_2$  are the inner and outer rays of the cylinder,  $d$  is the length of the cylinder, and  $\sigma$ , the specific conductivity of electrolyte solution. According to recent data (Conti et al., 1976) the mean values for *Rana pipiens* are:  $r_1 \simeq 10.68 \mu\text{m}$  and  $r_2 \simeq 15.34 \mu\text{m}$ .  $R_s$  was estimated to 40–100 K $\Omega$  for a surface of nodal membrane, varying from 22 (Cole, 1968) to 50  $\mu\text{m}^2$  (Conti et al., 1976) and  $\sigma = 10^{-2} \Omega^{-1} \text{cm}^{-1}$  in standard Ringer solution. When the bath solution is not the standard Ringer, the conductivity ( $\sigma$ ) modifies. For instance in the case of a D<sub>2</sub>O-Ringer solution, 30–40% decrease of  $\sigma$  is found at  $T = 18^\circ\text{C}$  which obviously induces an increased resistance of the nodal gap.

In Fig. 1 are shown also the values of the other circuit elements, regarded as standard values by some authors (Dodge and Frankenhaeuser, 1958; Nonner, 1969; Conti et al., 1976).

### COMPUTER SIMULATION

In order to simulate by computer the nodal gap effect on membrane currents, we considered the real case in which the voltage clamp was applied on the resistance of nodal gap in series

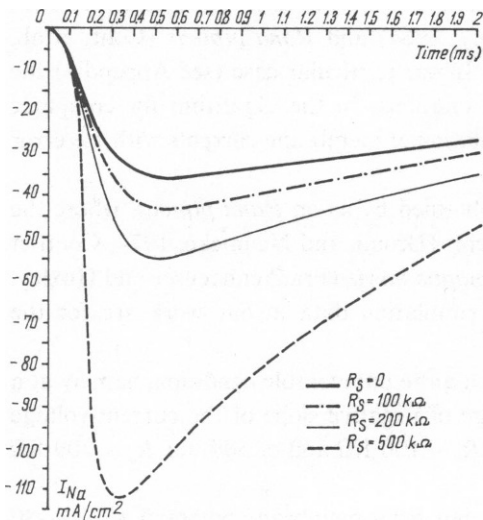


FIGURE 3

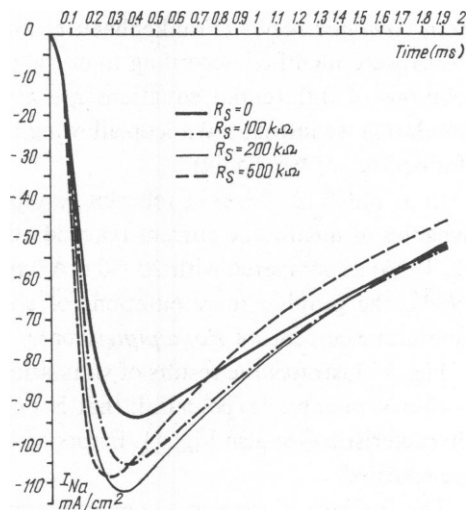


FIGURE 4

FIGURE 3 Computer simulation of the effect of nodal gap resistance measurements of ionic currents on the myelinated fiber of *Rana pipiens*; membrane potential  $V_m = -40 \text{ mV}$ ;  $I_{Na}$ , sodium current.

FIGURE 4 Computer simulation of the effect of nodal gap resistance in measurements of ionic currents of myelinated fiber of *Rana pipiens*; membrane potential  $V_m = -30 \text{ mV}$ ,  $I_{Na}$ , sodium current.

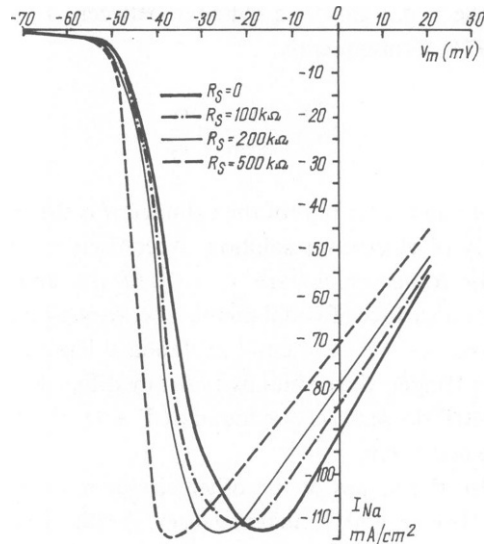


FIGURE 5 Current-voltage characteristics resulted for different series resistances in the computer simulation of the effect of nodal resistance in measurements of ionic currents on the myelinated fiber of *Rana pipiens*.

with the membrane impedance. A Felix C-256 (similar to IBM-360) digital computer was used (Electronic Computer Co., Bucharest, Romania).

The equations describing the membrane currents for two types of myelinated fiber taken from *Xenopus laevis* (Frankenhaeuser and Huxley, 1964) and *Rana pipiens* (Conti et al., 1976) were modified according to our hypothesis. In our particular case (see Appendix) the solutions of differential equations are analytical solutions. In the algorithm for computer simulation we introduced a loop allowing the calculation of membrane currents with 1% error (for details see Appendix).

In as much as the most relevant results were obtained by us on *Rana pipiens*, where the densities of membrane current reached 100 mA/cm<sup>2</sup> (Drouin and Neumcke, 1974; Conti et al., 1976) as compared with 20–30 mA/cm<sup>2</sup> on *Xenopus laevis* (Frankenhaeuser and Huxley, 1964), the graphic representations of computer simulation data in our work are for the membrane currents of *Rana pipiens* only.

Fig. 3 illustrates the results of simulation under a quite unfavorable condition, namely at a –40-mV membrane/potential; that is in the range of negative slope of the current-voltage characteristic (see also Fig. 5). Errors of 18% for  $R_s = 100 \text{ K}\Omega$  and of 50% for  $R_s = 200 \text{ K}\Omega$  are revealed.

The findings of the same computer simulation, but for a membrane potential  $V_m = -30 \text{ mV}$ , are shown in Fig. 4. Here nonlinear effects are evident and the errors of current values are greater at  $R_s = 200 \text{ K}\Omega$  than at  $R_s = 500 \text{ K}\Omega$ . Kinetic changes also occur.

Fig. 5 is a diagram of the current-voltage characteristics that result from plotting the maximum values of sodium current as a function of the membrane potential for various  $R_s$ . There is an obvious voltage shift due to the effect of the nodal gap resistance.

## CONCLUSIONS

On the basis of the results obtained by computer simulation the following conclusions may be drawn:

(a) The effect of the series resistance must not be overlooked in the measurements of the ionic currents on the Ranvier node membrane.

(b) The errors are maximum for the values of currents on the negative slope of the current-voltage characteristics (Fig. 3).

(c) At the estimated value  $R_s \approx 100 \text{ K}\Omega$  for the nodal gap resistance, errors of ~6–10% with *Xenopus Laevis* and 18–20% with *Rana pipiens* (Figs. 3 and 4) are found in the current amplitude.

(d) The errors may be still greater for a resistance value higher than that estimated by calculation, namely when the bath solution of the node membrane has a lower conductivity than that of the standard Ringer solution.

(e) Modifications also occur in the kinetics of ionic currents (see Fig. 4).

## APPENDIX

### *Equations Used for Computer Simulation of Sodium Currents in Rana Pipiens Myelinated Fiber*

For the case of voltage clamp the instantaneous sodium current could be described by the constant-field equation (Conti et al., 1976).

$$I_{Na} = P_{Na} [Na]_e \frac{V_m F^2}{RT} \frac{1 - \exp(V_m - V_{Na})F/RT}{1 - \exp V_m F/RT} \quad (1)$$

where  $F$ ,  $R$ ,  $T$  are the usual thermodynamic constants,

$$P_{Na} = m^3 h \bar{P}_{Na}, \quad (2)$$

$m$  and  $h$  are given by differential linear equations of the type

$$\frac{dK}{dt} = \alpha_K (1 - K) - \beta_K K \quad (3)$$

where  $K = m, h$ .

The velocity constants  $\alpha$  and  $\beta$  are obtained from the following equations (Conti et al., 1976):

$$\alpha_h = \frac{0.0119 (V_m + 72.5)}{\exp\left(\frac{V_m + 72.5}{7.38} - 1\right)} + 0.0005 \quad (4)$$

$$\beta_h = \frac{2}{\exp\left(-\frac{V_m + 10.5}{14.5}\right) + 1} \quad (5)$$

$$\alpha_m = \frac{0.366 (V_m + 37.5)}{1 - \exp\left(-\frac{V_m + 37.5}{3.8}\right)} + \frac{5.22}{1 + \left(\frac{V_m + 25}{18}\right)^2} \quad (6)$$

$$\beta_m = \frac{0.267 (V_m + 37.5)}{\exp\left(\frac{V_m + 37.5}{13.2}\right) - 1} \quad (7)$$

We also introduced the following values into our calculation.  $\bar{P}_{Na} = 5.31 \cdot 10^{-9} \text{ cm}^3 \text{ s}^{-1}$ ;  $V_{Na} = +60 \text{ mV}$ ;  $[Na]_e = 114.5 \text{ mM}$ . For the calculation of current densities a node membrane surface  $S_m = 30 \mu\text{m}^2$  was considered, and accordingly  $\bar{P}_{Na} = 17.7 \cdot 10^{-3} \text{ cm s}^{-1}$ .  $V_m$  is the absolute value of membrane potential (which varies from  $-70 \text{ mV}$  to  $+65 \text{ mV}$ );  $V$  is used for potentials relative to resting potential; thus  $V = V_m - V_R$  and  $V_R = -70 \text{ mV}$  (resting potential). Initial standard values (at  $V_m = V_R$ ) of the permeability variables  $m$  and  $h$  are:  $m_0 = 0.0005$ ,  $h_0 = 0.8249$ . To consider the effect of series resistance in Eqs. 1 and 4–7 we shall replace  $V_m$  by

$$V'_m = V_m - I_{Na} R_s \quad (8)$$

where  $R_s = 0; 100 \text{ K}\Omega; 200 \text{ K}\Omega; 500 \text{ K}\Omega$ .

In Eq. 8 the first value to be introduced for  $I_{Na}$  is the one resulting from Eqs. 1 and 4–7 for  $R_s = 0$ . By means of  $V'_m$  from Eq. 8 a new membrane current  $I'_{Na}$  will be calculated which in its turn will be used in the calculation of other potentials  $V''_m$ . These successive computations are performed by computer until the difference between two successive values of membrane current is  $< 1\%$ .

*Received for publication 2 December 1980 and in revised form 21 April 1981.*

## REFERENCES

- Binstock, L., J. W. Adelman, Jr., P. J. Senft, and H. Lecar. 1975. Determination of the resistance in series with the membrane of giant axons. *J. Membr. Biol.* 21:24–27.
- Cole, S. K. and H. Lecar. 1975. On the measurements of series resistance in giant axon preparations. *J. Membr. Biol.* 25:209–211.
- Conti, F., B. Hille, B. Neumcke, W. Nonner and R. Stämpfli. 1976. Measurement of the conductance of the sodium channel from current fluctuations at the node of Ranvier. *J. Physiol. (Lond.)* 262:699–727.
- Dodge, J., and B. Frankenhaeuser, 1958. Membrane currents in isolated frog nerve fibre under voltage clamp conditions. *J. Physiol. (Lond.)* 143:76–90.
- Drouin, H., and B. Neumcke. 1974. Specific and unspecific charges at the sodium channels of nerve membrane. *Pflügers Arch. Eur. J. Physiol.* 351:207–229.
- Frankenhaeuser, B., and F. A. Huxley. 1964. The action potential in myelinated nerve of *Xenopus Laevis* as computed on the basis of the voltage-clamp data. *J. Physiol. (Lond.)* 171:302–315.
- Hille, B. 1978. Ionic Channels in excitable membranes. *Biophys. J.* 22:283–294.
- Marmont, G. 1949. Studies of the new membrane. I. A new method *J. Cell. Comp. Physiol.* 34:351–382.
- Moore, W. J. 1978. On sodium conductance gate in nerve membrane. In *Physiology and Pathology of Axons*. S. G. Waxman, editor. Raven Press, New York. 145–153.
- Nonner, W. 1969. A new voltage clamp method for Ranvier nodes. *Pflügers Arch. Eur. J. Physiol.* 309:176–192.